HHS Public Access

Author manuscript

J Thromb Haemost. Author manuscript; available in PMC 2018 February 01.

Published in final edited form as:

J Thromb Haemost. 2017 February ; 15(2): 375–387. doi:10.1111/jth.13579.

In vitro characterization of SynthoPlate™ (synthetic platelet) technology and its in vivo evaluation in severely thrombocytopenic mice

Meenal Shukla[1], **Ujjal D S Sekhon**[2], **Venkaiah Betapudi**[1], **Wei Li**[1], **DaShawn A Hickman**[2], **Christa L Pawlowski**[2], **Mitchell R Dyer**[3], **Matthew D. Neal**[3], **Keith R McCrae**[1], and **Anirban Sen Gupta**[2,*]

[1]Cleveland Clinic Foundation, Department of Cellular and Molecular Medicine, Cleveland OH 44195, USA

[2]Case Western Reserve University, Department of Biomedical Engineering, Cleveland OH 44106, USA

[3]University of Pittsburgh Medical Center, Department of Surgery, Pittsburgh PA 15213, USA

Summary

Background—Platelet transfusion applications face severe challenges due to the limited availability and portability, high risk of contamination and short shelf-life of platelets. Therefore there is significant interest in synthetic platelet substitutes that can render hemostasis while avoiding these issues. Platelets promote hemostasis by injury site-selective adhesion and aggregation, and propagation of coagulation reactions on their membrane. Based on these mechanisms, we have developed a synthetic platelet technology (SynthoPlate™) that integrates platelet-mimetic site-selective 'adhesion' and 'aggregation' functionalities via heteromultivalent surface-decoration of lipid vesicles with Von Willebrand Factor-binding, collagen-binding and *active* platelet integrin GPIIb-IIIa-binding peptides.

Objective—SynthoPlate™ was evaluated for its effects on platelets and plasma in vitro, and for systemic safety and hemostatic efficacy in severely thrombocytopenic mice in vivo.

Methods—In vitro, SynthoPlate™ was evaluated using aggregometry, fluorescence microscopy, microfluidics, and thrombin and fibrin generation assays. In vivo, SynthoPlate™ was evaluated for systemic safety using prothrombin and fibrin assays on plasma and for hemostatic effect on tail-transection bleeding time in severely thrombocytopenic (TCP) mice.

*Corresponding author: Anirban Sen Gupta, PhD, Case Western Reserve University, Department of Biomedical Engineering, 10900 Euclid Avenue, Wickenden Bldg Rm 517B, Cleveland, OH 44106, Phone: 216-368-4564, anirban.sengupta@case.edu.

Addendum. A. Sen Gupta and K. R. McCrae directed research. U. D. D. S. Sekhon and C. L. Pawlowski prepared all particles, carried out mass spectroscopy and dynamic light scattering characterizations. D. A. Hickman, C. L. Pawlowski and W. Li carried out in vitro and ex vivo primary hemostasis and aggregometry studies. U. D. D. S. Sekhon carried out in vitro secondary hemostasis studies. M. Shukla, V. Betapudi, D. H. Hickman, M. Dyer and M. D. Neal carried out all in vivo studies in mice. A. Sen Gupta, K. R. McCrae, M. Shukla, C. L. Pawlowski, V. Betapudi, U. D. D. S. Sekhon and D. A. Hickman wrote the paper.

Disclosure of Conflict of Interest. A. Sen Gupta is inventor on patent related to SynthoPlate™ technology, ***US 9107845***. SynthoPlate™ trademark is currently recorded with USPTO.

Results—SynthoPlate™ did not aggregate resting platelets or spontaneously promote coagulation in plasma, but could amplify recruitment and aggregation of *active* platelets at the bleeding site and thereby site-selectively enhance fibrin generation. SynthoPlate™ dose-dependently reduced bleeding time in TCP mice, to levels comparable to normal mice. SynthoPlate™ has a reasonable circulation residence time and is cleared mostly by the liver and spleen.

Conclusion—The results demonstrate the promise of SynthoPlate™ as a synthetic platelet substitute in transfusion treatment of platelet-related bleeding complications.

Keywords

Bleeding Time; Haemostasis; Thrombocytopenia; Platelet Transfusion; Platelets

Introduction

Platelet transfusion is clinically important in the management of bleeding complications [1–4]. However, donor-derived platelets present issues of limited availability and portability, need for antigen matching, high risk of bacterial contamination and short shelf-life [5–9]. While robust research is being directed at resolving these issues, there is significant clinical interest in ‘donor-independent’ platelet technologies [10–13]. A promising research area in this aspect is ‘synthetic platelet substitutes’ [14]. To this end, we report on a ‘synthetic platelet’ technology (SynthoPlate™), whose design is based on mimicking platelet’s *primary hemostasis* mechanisms of injury site-specific *adhesion* (to collagen and Von Willebrand Factor) and *aggregation* (via fibrinogen-mediated bridging of integrin GPIIb-IIIa on *activated* platelets) [15–17]. Integration of these platelet-mimetic dual functionalities was achieved via heteromultivalent surface-decoration of biocompatible lipid vesicles with VWF-binding (VBP), collagen-binding (CBP) and active GPIIb-IIIa-binding Fg-mimetic peptides (FMP) (Fig 1) [18]. We have previously demonstrated that this integrative design results in superior hemostatic performance than ‘adhesion only’ and ‘aggregation only’ designs [19,20]. Also, in platelet’s hemostatic action, co-localization of coagulation factors on the surface of activated pro-coagulant platelets at the bleeding site results in amplification of thrombin and fibrin generation (*secondary hemostasis*) [21]. Thus, we hypothesized that SynthoPlate™ mediated direct enhancement of platelet *recruitment* and *aggregation* at an injury site would in effect also enhance secondary hemostatic output at that site (envisioned mechanism in Fig S.1). Therefore, here we focused on characterizing the capabilities of SynthoPlate™ vesicles regarding primary and secondary hemostatic mechanisms in vitro, and subsequently evaluated the systemic safety and hemostatic efficacy of SynthoPlate™ in vivo in a mouse model of thrombocytopenia [22].

Materials and Methods

Materials

Distearylphosphatidyl choline (DSPC), carboxy-poly(ethylene glycol)-modified distearylphosphatidyl ethanolamine (DSPE-PEG_{2000}-COOH) and Rhodamine-B-dihexadecanoyl-sn-glycero-3-phosphoethanolamine (DHPE-RhB) were from Avanti Polar

Lipids (Alabaster, AL). The peptides TRYLRIHPQSWVHQI (**VBP**), $[GPO]_7$ (**CBP**), and cyclo-CNPRGDY(OEt)RC (**FMP**) were custom-synthesized from Genscript (Piscataway, NJ USA) conjugated to DSPE-PEG_{2000}-COOH and characterized by mass spectrometry (Fig S. 2). Phosphate-buffered saline (PBS), bovine serum albumin (BSA), sodium bicarbonate and fluorescent human fibrinogen (Alexa Fluor-647-labeled) were from Thermo Fisher (Pittsburgh, PA). Cholesterol and rat tail Type I collagen were from Sigma Aldrich (Saint Louis, MO), Adenosine Diphosphate (ADP) from Bio/Data Corporation (Horsham, PA, USA) and Human VWF (FXIII-free) from Hematologic Technologies (Essex Junction, VT). Citrated human whole blood was obtained from freshly donated stock from healthy donors at Case School of Medicine. The parallel plate flow chamber (PPFC) system was from Glycotech (Gaithersburg, MD). For mouse studies, MOPC-21, anti-CD41 and anti-CD42 antibodies were obtained from Abcam (Cambridge, MA). For immunostaining, rat anti-mouse CD41 antibodies were from BioRad (Hercules, CA), FITC-labeled donkey-anti-rat IgG from Thermo-Fisher (Waltham, MA), rat anti-mouse CD31 from Biolegend (San Diego, CA) and goat anti-rat AlexaFluor 633-IgG from Thermo-Fisher. For immunoblot studies, lysis buffer (RIPA) was obtained from Sigma-Aldrich, protease inhibitors from Roche Applied Science (Madison, WI), phosphatase inhibitors and aprotinin from Sigma-Aldrich, corn trypsin inhibitor from Haematologic Technologies, Protein DC assay from Bio-Rad (Hercules, CA), rabbit polyclonal fibrinogen/fibrin antibody from Life Span Biosciences (Seattle, WA), HRP-conjugated secondary antibody from Cell Signaling (Danvers MA), super signal west Pico chemiluminiscent substrate from Thermo Fisher (Waltham MA) and antibodies to beta actin from SantaCruz Biotechnology (Santa Cruz, CA). All in vivo studies were carried out per approved IACUC protocols at Cleveland Clinic and University of Pittsburgh.

Manufacture of SynthoPlate^{TM}

The SynthoPlate^{TM} design leverages a clinically relevant poly(ethylene glycol)-modified lipid vesicle platform, refined by heteromultivalent ligand decoration [23]. For this, DSPC, cholesterol, DSPE-PEG-VBP, DSPE-PEG-CBP and DSPE-PEG-FMP were homogenously mixed at mole fractions of 0.50, 0.45, 0.0125, 0.0125 and 0.025 respectively in 1:1 methanol:chloroform and this lipid mixture was exposed to reverse phase evaporation, PBS-based hydration and subsequent extrusion through 200nm pore-size membrane (Northern Lipids Inc.) to yield heteromultivalently surface-decorated SynthoPlate^{TM} vesicles (schematic in Fig 1A). Dynamic light scattering (DLS), scanning electron microscopy (SEM) and cryo-Transmission Electron Microscopy (cryo-TEM) characterization indicated vesicles of ~150 nm diameter (Fig 1, B, C and D). Based on these parameters, the theoretical ligand density per vesicle is ~50,000 (Supporting Information Section S.3). Using a Malvern zetasizer, the zeta potential of SynthoPlate^{TM} was found to be −24.9 +/− 8.00 mV and that for control (unmodified) particles −25.2 +/− 9.77 mV.

In vitro studies of SynthoPlate^{TM} effect on platelet aggregation

Turbidimetric experiments were carried out with platelet-rich plasma (PRP) using ADP as agonist or washed platelets (Plts) using collagen as agonist, utilizing a Chrono-log Aggregometer (Havertown, PA), to test the interaction of SynthoPlate^{TM} with active versus resting platelets. Wild type C57Bl-6 mice were anesthetized and whole blood was drawn

through venipuncture using 0.109 M sodium citrate. Modified Tyrode's buffer (0.7 v/v) was added and PRP was separated by centrifugation. Platelet concentration in PRP was adjusted to 2.50E+08/ml with platelet-poor plasma (PPP). To prepare washed platelets, PRP was further centrifuged at 650 g for 6 min in the presence of 0.5 μM PGE1. Resultant platelet pellet was resuspended in PBS containing 0.109 M sodium citrate (9:1, v/v) and 0.5 μM PGE1, re-pelleted and resuspended in PBS to a concentration of 2.50E+08/ml. Aggregometry studies were conducted at 37°C with stirring at 1200 rpm. ADP-mediated aggregation was performed using 400 μl PRP (labeled as 100% PRP in Fig 2A), or PRP diluted 50% (v/v) with either PPP (50% PRP in Fig 2A) or PPP containing SynthoPlate™ or PPP containing control particles with particle concentration at 5.00E+10/ml. To further ensure that the effects of SynthoPlate™ (or control particles) was specifically on platelets, collagen-based aggregation studies was performed using washed platelets instead of PRP (labeled as 100% Plts or 50% Plts in Figure 2B), and here particles were suspended in PBS instead of PPP. Aggregation was monitored adding a final concentration of 1 mM Ca^{++}/Mg^{++} and, with or without addition of platelet agonists (ADP at 2.5 μM and collagen at 1μg/ml). The 50% dilution of platelets was considered as a thrombocytopenic condition rationalizing from clinical definition [24]. The same SynthoPlate™ and control particles were also used to characterize the particle-mediated recruitment and aggregation of active platelets on 'VWF + collagen'-coated surfaces under flow in the PPFC, imaged under fluorescence microscopy. For this, calcein-stained (green fluorescent) platelets suspended in plasma (50,000/ml) were flowed over 'VWF + collagen'-coated surfaces along with RhB-labeled (red fluorescence) SynthoPlate™ (or control) particles, ADP (2.5 μM) and soluble VWF (10μg/ml), adapting previously published methodology [25, 26]. The flow was maintained at shear stress of 50 dyn/cm^2 (shear rate >3000 sec^{-1} assuming plasma as Newtonian fluid with constant viscosity of 0.015 Poise) to ensure hemostatically relevant interaction of VWF with collagen [27]. The co-localization of active platelets (green) and particles (red) on the surfaces was imaged using a Zeiss inverted fluorescence microscope (schematic [A] in Fig S.4).

In vitro studies of SynthoPlate™ effect on thrombin and fibrin generation

Experiments were carried out to first study whether SynthoPlate™ vesicles themselves spontaneously generate thrombin in human plasma (i.e. assessing systemic coagulation risk). PRP was obtained from freshly drawn citrated human whole blood by centrifugation (150g, 15 min) and PPP was obtained by further centrifuging PRP (2500g, 20 min). The thrombin-cleavable fluorogenic substrate (p-tosyl-Gly-Pro-Arg)$_2$-Rhodamine-110 (Thermo Fisher) at final concentration of 0.1 mM (in Tris buffer, pH 7.4, 22°C) was incubated in presence of 5% v/v 0.5M $CaCl_2$ with the groups: 'PPP only', 'PRP only', 'PPP + SynthoPlate™', 'PRP + SynthoPlate™', 'PPP + Tissue Factor', 'PRP + Tissue Factor' 'PRP + SynthoPlate™ + Tissue Factor', 'PRP + ADP + Tissue Factor', 'PRP + ADP + SynthoPlate™ + Tissue Factor'. Particle concentration, in groups applicable, was 5.00E+10/ml. The resultant thrombin activity was monitored using a Bio-Tek plate reader (excitation/emission at 498/521 nm) for 40 min. Next, for fibrin generation/deposition studies, the PPFC set-up was used as before with some modifications. Glass slides pre-coated with 'collagen + VWF' or BSA were sealed within the PPFC and exposed to flow of fresh 100% PRP (platelet count 250,000 per μl), or 50% PRP (platelet count diluted 50% with PPP to 125,000 per μl), or

100% PPP and SynthoPlate™ (or control) particles, in presence of fluorescent fibrinogen (Alexa Fluor 647-Fg at 1.5 mg/ml added at 3% v/v), with or without ADP. The 'control' particles had only pro-adhesive peptides (VBP and CBP only, no FMP) such that they can still bind to the 'vWF + collagen' substrate but cannot recruit and aggregate active platelets. The flow was maintained at 50 dyn/cm^2 for 15 min. In this set-up, SynthoPlate™-mediated recruitment and aggregation of active platelets on the 'VWF + collagen' surface was hypothesized to augment the availability of pro-coagulant active platelet membrane for facilitating secondary hemostatic mechanisms, leading to amplified generation and deposition of fibrin(ogen) during the 15 min time-window (experiment schematic Fig S.5). This deposition was imaged with inverted fluorescence microscopy (emission 665 nm). At 15 min the flow was stopped and the clots on the slides were incubated with Streptokinase (SK) in PPP (20 μl per ml of PPP) for 60 min. Resultant lysed clots were analyzed with fibrin D-dimer-specific spectrophotometric ELISA assay (Thermo Fisher) as per manufacturer instructions and D-dimer levels were calculated using a standard calibration curve. The D-dimer analysis was to confirm that the clot fluorescence observed was indeed from fibrin generation and not just fibrinogen.

Effect of SynthoPlate™ in severely thrombocytopenic (TCP) mice

We adapted a model of passive immune thrombocytopenia (ITP) in mice with platelet-specific antibodies [28]. Wild-type C57/BL6 mice were injected intraperitoneally with a combination of anti-CD41 and anti-CD42 antibodies (1:1 ratio at 1–10 μg total) and 24 hr later platelet counts were measured using an Advia 120 Hematology analyzer (6 mice per group). For bleeding time assessment, 24 hr after 10 μg antibody administration, tails of thrombocytopenic mice were transected 2 mm from the tip with a surgical blade, immersed in 37°C saline, and the time for bleeding to stop was recorded (schematic in Fig 4A) [29]. Next, similarly treated TCP mice were injected with 150 μl of various doses (100/nL, 500/nL or 1000/nL) of SynthoPlate™ or control (unmodified) particles via jugular vein and 2 hours after particle injection the mouse tails were transected as before to record bleeding time. The 2 hr circulation time-period was chosen as a feasibility metric for evaluating the 'prophylactic window' of the SynthoPlate™ technology and future studies will focus on expanding this window to longer circulation lifetimes. All tail-bleeding studies were performed in accordance with standardization parameters highlighted by ISTH [30]. After bleeding time studies, mice were sacrificed, 4–5mm tail-pieces proximal to transection site were cut, washed in PBS, fixed in paraformaldehyde for 24 hours and then cryoprotected in 30%–60% sucrose and flash frozen in O.C.T. compound (Tissue Tek®, Torrance CA). Cryoblocks were prepared in cryo-molds (Electron Microscopy Sciences, Hatfield PA) over dry ice and 2-methyl butane, and 9 μm thick sections were cut using a Leica CM1950 cryostat and collected on super-frost glass slides (Thermo-Fisher) for staining. For immunostaining, frozen sections were air-dried, rinsed in PBS and blocked with 0.1% Tween-20 and 1% BSA. A sequential staining protocol was followed in which sections were first incubated with rat anti-mouse CD41 antibodies overnight at 4° C, followed by washing in PBS and incubation with a FITC-labeled donkey-anti-rat IgG for 2 hours. After additional washes, sections were incubation with rat anti-mouse CD31 for 2 hours, then washed and labeled with goat anti-rat AlexaFluor 633-IgG. Slides were mounted with Vectashield and imaged under a Leica fluorescent microscope.

In additional experiments, similar tail sections from thrombocytopenic mice treated with SynthoPlate™ or control particles, were collected directly into lysis buffer containing protease inhibitors, phosphatase inhibitors, corn trypsin inhibitor and aprotinin. Tails were disrupted by sonication, and lysates clarified by centrifugation at 12000 rpm for 15 min at 4°C. The supernatant was collected and protein was measured using the Protein DC assay. For immunoblotting, tail extracts were mixed with 5X SDS sample buffer containing beta-mercaptoethanol and heated at 95°C for 5 min. Samples were resolved on 10% SDS-PAGE by loading 25 μg of protein in each lane, and transferred to PVDF. Membranes were probed overnight at 4°C with a 1:5000 dilution of rabbit polyclonal fibrinogen/fibrin antibody (Life Span Biosciences, Seattle, WA). Bound antibody was detected using an HRP-conjugated secondary antibody and super signal west Pico chemiluminescent substrate. The membrane was stripped in stripping buffer containing 15 g/L glycine, 1 g/L SDS, and 10 ml/L Tween-20, pH 2.2, blocked and re-probed using antibodies to beta actin.

Assessing systemic safety and biodistribution of SynthoPlate™ during 2 hr circulation

For systemic safety analysis, wild-type or TCP mice were intravenously injected with SynthoPlate™ or control (unmodified) particles and 2 hours after particle injection blood was collected via cardiac puncture in sodium citrate (0.109M, 3.2%) and analyzed with an immuno-turbidimetric agglutination assay for circulating fibrin D-Dimer levels (STA-Liatest D-Di, Diagnostica Stago, USA) per manufacturer's instructions [31]. In parallel experiments, mice were injected intravenously with 8 μg/kg LPS (positive control) or 120 μl of SynthoPlate™ or control particles (1000/nl). At 30 min and 2 hrs after injection, blood was drawn from the facial vein directly into tubes containing sodium citrate, corn trypsin inhibitor and aprotinin, centrifuged at room temperature for 10 min at 2500 rpm and the plasma collected and analyzed with a double-antibody sandwich ELISA for prothrombin fragment 1+ 2 per the manufacturer's instructions (Biosource, San Diego, CA).

For biodistribution studies, mice were injected intravenously with SynthoPlate™ and euthanized after 2 hr with overdose of anesthesia cocktail. Various organs were harvested, rinsed in PBS and freeze-dried to obtain dry weight. The organs were homogenized at 4000rpm (BeadBug Microtube Homogenizer, Benchmark Scientific, Edison, NJ), and homogenates were shaken overnight at 750rpm 37°C with 1:1 methanol/chloroform solution to extract the RhB-labeled lipids. Resultant samples were centrifuged at 3,000rpm for 10 minutes, the supernatant containing RhB-labeled lipids were collected and fluorescence in the supernatant was determined using a Bio-Tek Plate reader (excitation 550nm, emission 590nm). The SynthoPlate™ percentage in various organs was determined by calculating the concentration (ng/ml) of particles in supernatant from a calibration curve. In complementary studies, SynthoPlate™ particles were radiolabeled either by incorporating tritium (^{3}H)-tagged cholesteryl ester in the vesicle membrane or encapsulating Indium Chloride ($^{111}InCl_3$) in the vesicle core (representative results in Fig S.6). Following tail-vein injection of these particles in mice, animals were either sacrificed to harvest organs and blood for scintillation counting of ^{3}H-labeled particles or whole-body imaged by Single Photon Emission Computed Tomography (SPECT-CT) for assessing $^{111}InCl_3$-labeled particle distribution.

Statistical analysis

Where applicable, data were expressed as mean ± SD. Aggregometry results were analyzed by 1-way ANOVA with Bonferroni post-hoc test for multiple comparisons with SigmaStat 3.5. Thrombin and fibrin assay results were analyzed by 1-way ANOVA and Tukey's test. For some in vivo results, analyses were also carried out by 2-tailed Student's t-test. $P<0.05$ were considered statistically significant.

Results

In vitro studies of SynthoPlate^{TM}-mediated primary hemostasis mechanisms

Representative aggregometry data for PRP or washed platelets, along with corresponding histograms of percent (%) aggregation, are shown in Fig 2A1–A2 and 2B1–B2 respectively. As evident from Fig 2A1, without platelet activation, SynthoPlate^{TM} itself has no aggregatory effect on platelets, since the turbidimetric trace for this (brown) was same as that for resting (w/o ADP) platelets (indigo). This suggests that SynthoPlate^{TM} will not activate resting platelets in the circulation. Upon agonist addition, platelet aggregation was observed in 100% PRP as well as 100% Plts (green traces in Fig 2A1 and 2B1). This aggregation was significantly reduced when PRP was diluted by 50% v/v with PPP or Plts by saline (purple traces in Fig 2A1 and 2B1). This dilution effect was not rescued when control (unmodified) particles were added (red traces in Fig 2A1 and 2B1). In contrast, addition of SynthoPlate^{TM} particles could significantly rescue the aggregation (cyan traces in Fig 2A1 and 2B1). Statistical analyses (Fig 2A2 and 2B2) clearly depict this ability of SynthoPlate^{TM} to improve the aggregation of diluted platelets. Also, the SynthoPlate^{TM} vesicles themselves do not have any aggregation in presence of platelet agonists and Ca^{++} (Fig S.7). Fluorescence microscopy studies in PPFC showed that RhB-labeled (red fluorescent) SynthoPlate^{TM} particles have significant co-localization (yellow overlay) with calcein-stained (green fluorescent) active platelets on a 'VWF + collagen' surface, while unmodified, 'adhesion only' and 'aggregation only' particles have minimal co-localization (Fig S.4.B). These results are in accordance to our previously reported findings [19, 20]. Altogether, these studies indicate: (i) SynthoPlate^{TM} interacts specifically with activated platelets to augment their aggregation, and, (ii) this aggregation can be enhanced selectively at the site of 'vWF + collagen' exposure (amplification of primary hemostasis) via SynthoPlate^{TM} action.

In vitro studies of SynthoPlate^{TM}-mediated thrombin generation

Fig 3A shows the table for thrombin generation parameters obtained for the various groups studied. As evident from the results, without TF or platelet agonist (ADP), adding SynthoPlate^{TM} in re-calcified PRP or PPP does not induce and accelerate rapid thrombin generation and thrombin generation occurs with a much longer lag time as common for re-calcified plasma [32]. In presence of TF and/or ADP, thrombin generation is drastically accelerated in PRP (or PPP) even without SynthoPlate^{TM} and the reaction speed increases slightly when SynthoPlate^{TM} is present. This indicates that SynthoPlate^{TM} itself does not *directly* influence thrombin generation in plasma, but can possibly *indirectly* influence thrombin generation if it can recruit pro-coagulant active platelets at the site of injury and TF exposure. This possibility is further confirmed in the fibrin(ogen) generation/deposition

study results under flow (representative images and quantitative results in Fig 3B and 3C). In this case, during the 15 min time-window, the fluorescence of deposited fibrin(ogen) significantly increases when ADP-activated 50% PRP is flowed with SynthoPlate™ over 'vWF + collagen' surface, compared to the control conditions. The D-dimer ELISA studies further confirm that the deposited clot in this group contains a significant amount of fibrin (Fig 3D). These studies altogether confirm that SynthoPlate™ does not have any innate ability to stimulate coagulation in plasma (therefore, minimum systemic pro-coagulant risk), but can 'in effect' augment coagulatory output at the injury site by enhancing the recruitment and aggregation of *active* platelets at the site.

Severe thrombocytopenia induction in mice and effect of SynthoPlate™ on tail bleeding

Fig 4A1 shows the platelet count following antibody treatment, demonstrating that a total dose of 10μg antibody combination (5μg each) resulted in ~90% reduction of platelet count (severe thrombocytopenia). Injection of PBS or non-specific mouse IgG (MOPC-21) did not deplete platelets. The effect of platelet depletion on the hemostatic capacity of mice is shown in Fig 4A2, where 10μg antibody injection (i.e. platelet depletion by ~90%) resulted in 4–5 fold increase in tail-bleeding time. This severe thrombocytopenia (TCP) condition was subsequently used to test the capability of prophylactically administered SynthoPlate™ to improve hemostasis. Fig 4B shows the effect of SynthoPlate™ versus control particle treatment on tail-bleeding time in TCP mice. As evident, PBS alone or control particles were unable to correct the prolonged bleeding time (400–500 seconds). In contrast, SynthoPlate™ was able to significantly correct the bleeding time in a dose-dependent manner. The highest dose of SynthoPlate™ (1000/nL, equivalent to murine native platelet concentration) could reduce the bleeding time to ~150 seconds (>60% reduction compared to controls), close to that of normal mice (~100 sec, shown for comparison). These studies demonstrate that SynthoPlate™ could efficiently correct the hemostatic defect in thrombocytopenia. Fig 5A and 5B show representative immunofluorescence images of cryo-sectioned tail tissue immediately proximal to the tail transection site, showing vascular endothelium (CD31 in blue), particle fluorescence (red), platelets (CD41 in green), and corresponding overlays, for SynthoPlate™-treated versus control particle-treated TCP mice respectively. Fig 5C shows the percentage (%) of vasculature that demonstrated co-localization of CD41 (platelets) and SynthoPlate™ (or control) particles, determined from 24 representative images per injection group (6 mice per group) by manual counting. These images clearly indicate that compared to control (unmodified) particles, SynthoPlate™ has significantly greater ability to enhance recruitment and aggregation of platelets in the injured vessels in TCP mice. Fig 5D shows representative immunoblot data (for fibrin/fibrinogen as well as beta-actin as a loading control), for tail-tissue from SynthoPlate™-treated versus control particle-treated TCP mice. Individual fibrinogen α, β and γ chains are not well resolved, but are seen as prominent bands of ~45–63 kDa. However, higher molecular weight bands, consistent with thrombin-cleaved cross-linked fibrin, are apparent in the SynthoPlate™-treated (lanes 3 and 4), but not detected in control particle-treated mice (lanes 1 and 2). These results further indicate that in TCP mice, SynthoPlate™-mediated platelet recruitment and aggregation at the injury site (amplification of primary hemostasis) also enhances thrombin generation and fibrin deposition at the site (secondary hemostasis) to improve overall hemostatic capability.

Systemic safety and biodistribution of SynthoPlate™ during 2 hr circulation

Fig 6A shows 30 min and 2 hr time-point results for ELISA-based analysis of prothrombin fragment 1+ 2 in SynthoPlate™-injected mice (untreated mice or LPS-injected mice as controls). SynthoPlate™ did not enhance prothrombin fragment levels, indicating their minimum pro-coagulant activity in plasma. This is further validated by the Stago D-dimer assay results shown in Fig 6B where neither control nor TCP mice were found to have enhanced levels of fibrin D-dimer in the systemic circulation at the 2hr time point following SynthoPlate™ or control particle administration (compared to manufacturer-supplied controls). These in vivo results, combined with previous in vitro assays, further establish that SynthoPlate™ does not have systemic pro-thrombotic and pro-coagulant effects. Fig 6C shows representative cryosection fluorescence images of tissues from various clearance organs harvested from euthanized mice at the 2 hr time point and Fig 6D shows the percent (%) localization of SynthoPlate™ particles (based on RhB fluorescence) analyzed from homogenates of such organs. During the 2-hr circulation period only ~15% of the injected dose was cleared, mostly in liver and spleen and minimally in other organs. This suggests that the majority of the dose remained in the circulation to facilitate hemostasis in the event of injury. In fact, complementary studies using radiolabeled particles (representative data in Fig S.6) further indicate that SynthoPlate™ has a reasonably long circulation residence time. Since SynthoPlate™ design leverages polyethylene glycol (PEG)-decorated lipid vesicles, this long circulation capability and low clearance is in good agreement with reports for similar nanoparticles (e.g. Stealth liposomes) [23].

Discussion

Synthetic platelet substitutes can potentially resolve many issues that currently complicate platelet transfusion [13, 14, 33, 34]. Several past ‘synthetic platelet’ designs have focused on amplifying the ‘platelet aggregation’ mechanism by coating synthetic particles with fibrinogen (Fg) or Fg-relevant peptides, but have not yet translated into clinical application [35–37]. We rationalized that promoting platelet aggregation without a synergistic mechanism of bleeding site-selective adhesion may pose systemic pro-thrombotic risks from free-floating aggregates. Therefore, we have developed a synthetic platelet technology (SynthoPlate™) that combines platelet-mimetic *adhesion* and *aggregation* functionalities on a biocompatible lipid vesicle and have previously demonstrated the advantage of this integrative design in vitro and in vivo in normal mice [19, 20]. Building on these findings, in our current studies we established that the SynthoPlate™ vesicles themselves do not have systemic pro-thrombotic or pro-coagulant risks, but can amplify *activated* platelet-mediated primary and secondary hemostatic mechanisms selectively at a bleeding site, even at low platelet concentrations. Our in vivo studies further confirmed that prophylactic administration of SynthoPlate™ can dose-dependently improve hemostasis in a tail-bleeding model in severely thrombocytopenic mice, with higher doses capable of correcting bleeding times to levels comparable to that of normal mice. One should note that the starting platelet count in normal mice (~1 million per microliter) is significantly higher than normal human (~250,000 per microliter), and hence the severity of thrombocytopenic bleeding risk in mice is associated with the percent (%) platelet depletion and not the absolute number of remaining platelet count. Also, since tail-bleeding studies may have some experimental

heterogeneity, we have meticulously followed the ISTH standardization recommendations for this model to minimize errors and variabilities [30]. Immunofluorescence microscopy and immunoblot analyses confirmed striking co-localization of murine platelets and SynthoPlate^{TM}, as well as enhanced formation of fibrin in hemostatic foci of SynthoPlate^{TM}-injected mice. In vivo, SynthoPlate^{TM} vesicles showed reasonably long circulation periods and were primarily cleared by the liver and spleen. The SynthoPlate^{TM} technology may also find potential uses in emergency treatment of traumatic hemorrhage, and as a targeted drug delivery platform in various platelet-relevant diseases [38–40].

Supplementary Material

Refer to Web version on PubMed Central for supplementary material.

Acknowledgments

This work was supported by the National Institutes of Health, specifically by the National Heart Lung and Blood Institute (NHLBI) under award numbers **R01 HL121212** (PI: Sen Gupta) and **R01 HL089796** (PI: McCrae) as well as, by the National Institute of General Medical Sciences (NIGMS) under award number R35 GM119526 (PI: Neal, Co-I: Sen Gupta). The authors acknowledge Jaqueline Wallat and Sergey Isarov at Case Western for help with MALDI-TOF, Rekha Srinivasan at Case Western for help with SEM, and Emre Filrar and Tolou Shokuhfar at University of Illinois Chicago for help with Cryo-TEM. The content of this publication is solely the responsibility of the authors and does not necessarily represent the official views of the National Institutes of Health.

References

1. Kaufman RM, Djulbegovic B, Gernsheimer T, Kleinman S, Tinmouth AT, Capocelli KE, Cipolle MD, Cohn CS, Fung MK, Grossman BJ, Mintz PD, O'Malley BA, Sesok-Pizzini DA, Shander A, Stack GE, Webert KE, Weinstein R, Welch BG, Whitman GJ, Wong EC, Tobian AAR. Platelet Transfusion: A Clinical Practice Guideline From the AABB. Ann Intern Med. 2015; 162:205–13. [PubMed: 25383671]
2. Mohanty D. Current concepts in platelet transfusion. Asian J Transfus Sci. 2009; 3:18–21. [PubMed: 20041092]
3. Holcomb JB. Optimal use of blood products in severely injured trauma patients. Hematology Am Soc Hematol Educ Program. 2010:465–69. [PubMed: 21239837]
4. Babic, A., Kaufman, RM. Principles of platelet transfusion therapy. In: Hoffman, R.Benz, EJ.Shattil, SJ.Furie, B.Silberstein, LE., Heslop, H., editors. Hematology: Basic Principles and Practice. Churchill Livingstone; Philadelphia: 2009. p. 2219-23.
5. Solheim BG. Pathogen reduction of blood components. Transfus Apher Sci. 2008; 39:75–82. [PubMed: 18602343]
6. Stanworth SJ, Navarrete C, Estcourt L, Marsh J. Platelet refractoriness - practical approaches and ongoing dilemmas in patient management. Br J Haematol. 2015; 171:297–305. [PubMed: 26194869]
7. Blajchman MA. Immunomodulatory effects of allogeneic blood transfusions: clinical manifestations and mechanisms. Vox Sang. 1998; 74:315–19. [PubMed: 9704462]
8. Slichter SJ. Platelet refractoriness and alloimmunization. Leukemia. 1998; 12:S51–53. [PubMed: 9777897]
9. Kaiser-Guignard J, Cenellini G, Lion N, Abonnenc M, Osselaer JC, Tissot JD. The clinical and biological impact of new pathogen inactivation technologies on platelet concentrates. Blood Reviews. 2104; 28:235–41.
10. Spitalnik SL, Triulzi D, Devine DV, Dzik WH, Eder AF, Gernsheimer T, Josephson CD, Kor DJ, Luban NL, Roubinian NH, Mondoro T, Welniak LA, Zou S, Glynn S. 2015 proceedings of the National Heart, Lung, and Blood Institute's State of the Science in Transfusion Medicine symposium. Transfusion. 2015; 55:2282–90. [PubMed: 26260861]

11. Lambert MP, Sullivan SK, Fuentes R, French DL, Poncz M. Challenges and promises for the development of donor independent platelet transfusions. Blood. 2013; 121:3319–24. [PubMed: 23321255]
12. Thon JN, Mazutis L, Wu S, Sylman JL, Ehrlicher A, Machlus KR, Feng Q, Lu S, Lanza R, Neeves KB, Weitz DA, Italiano JE Jr. Platelet bioreactor-on-a-chip. Blood. 2014; 124:1857–67. [PubMed: 25606631]
13. Blajchman MA. Substitutes for success. Nature Med. 1999; 5:17–18. [PubMed: 9883829]
14. Modery-Pawlowski CL, Tian LL, McCrae KR, Mitragotri S, Sen Gupta A. Approaches to synthetic platelet analogs. Biomaterials. 2013; 34:526–41. [PubMed: 23092864]
15. Hoffman M, Monroe DM III. A cell-based model of hemostasis. Thromb Haemost. 2001; 85:958–65. [PubMed: 11434702]
16. Ni H, Freedman J. Platelets in hemostasis and thrombosis: role of integrins and their ligands. Transfus Apher Sci. 2003; 28:257–264. [PubMed: 12725952]
17. Versteeg HH, Heemskirk JWM, Levi M, Reitsma PH. New fundamentals in hemostasis. Physiol Rev. 2013; 93:327–358. [PubMed: 23303912]
18. Sen Gupta, A., Ravikumar, M. US Patent: Synthetic Platelets. US 9107845. 2015.
19. Modery-Pawlowski CL, Tian LL, Ravikumar M, Wong TL, Sen Gupta A. In vitro and in vivo hemostatic capabilities of a functionally integrated platelet-mimetic liposomal nanoconstruct. Biomaterials. 2013; 34:3031–41. [PubMed: 23357371]
20. Anselmo AC, Modery-Pawlowski C, Menegatti S, Kumar S, Vogus DR, Tian LL, Chen M, Squires TM, Sen Gupta A, Mitragotri S. Platelet-like Nanoparticles: Mimicking shape, flexibility, and surface biology of platelets to target vascular injuries. ACS Nano. 2014; 8:11243–53. [PubMed: 25318048]
21. Mann KG, Brummel-Ziedins K, Orfeo T, Butenas S. Models of blood coagulation. Blood Cells Molecules and Diseases. 2006:108–117.
22. Quillen, K., Bakdash, S. Chapter 12: Transfusion Medicine. American Society of Hematology Self-Assessment Program. 5ASH-SAP.org
23. Immordino ML, Dosio F, Cattel L. Stealth liposomes: review of the basic science, rationale, and clinical applications, existing and potential. Int J Nanomed. 2006; 1:297–315.
24. Veneri D, Franchini M, Randon F, Nichele I, Pizzolo G, Ambrosetti A. Thrombocytopenias: a clinical point of view. Blood Transfus. 2009; 7:75–85. [PubMed: 19503627]
25. Stevens JM. Platelet adhesion assays performed under static conditions. Methods Mol Biol. 2004; 272:145–51. [PubMed: 15226542]
26. Ravikumar M, Modery CL, Wong TL, Sen Gupta A. Peptide-decorated liposomes promote arrest and aggregation of activated platelets under flow on vascular injury relevant protein surfaces in vitro. Biomacromolecules. 2012; 13:1495–1502. [PubMed: 22468641]
27. Di Stasio E, De Cristofaro R. The effect of shear stress on protein conformation. Physical forces operating on biochemical systems: The case of von Willebrand factor. Biophys Chem. 2010; 153:1–8. [PubMed: 20797815]
28. Morowski M, Vögtle T, Kraft P, Kleinschnitz C, Stoll C, Newswandt B. Only severe thrombocytopenia results in bleeding and defective thrombus formation in mice. Blood. 2013; 121:4938–47. [PubMed: 23584880]
29. Turecek PL, Gritsch H, Richter G, Auer W, Pichler L, Schwarz HP. Assessment of bleeding for the evaluation of therapeutic preparations in small animal models of antibody-induced hemophilia and von Willebrand disease. Thromb Haemost. 1997; 77:591–99. [PubMed: 9066015]
30. Greene TK, Schiviz A, Hoellriegel W, Poncz M, Muchitsch E-M. on behalf of the animal models subcommittee of the scientific and standardization committee of the ISTH. Towards a standardization of the murine tail bleeding model. J Thromb Haemost. 2010; 8:2820–2. [PubMed: 21138523]
31. Baumgartner CK1, Mattson JG1, Weiler H1, Shi Q, Montgomery RR. Targeting Factor VIII expression to platelets for hemophilia A gene therapy does not induce an apparent thrombotic risk in mice. J Thromb Haemost. 2016; Epub ahead of print. doi: 10.1111/jth.13436

32. Altman R, Scazziota AS, Herrera Md-L, Gonzalez C. Thrombin generation by activated factor VII on platelet activated by different agonists. Extending the cell-based model of hemostasis. Thrombosis Journal. 2006; :4.doi: 10.1186/1477-9560-4-5 [PubMed: 16504043]

33. Lashof-Sullivan M, Shoffstall A, Lavik E. Intravenous hemostats: challenges in translation to patients. Nanoscale. 2013; 5:10719–28. [PubMed: 24088870]

34. Chan LW, White NJ, Pun SH. Synthetic strategies for engineering intravenous hemostats. Bioconjugate Chem. 2015; 26:1224–36.

35. Levi M, Friederich PW, Middleton S, de Groot PG, Wu YP, Harris R, Biemond BJ, Heijnen HF, Levin J, ten Cate JW. Fibrinogen-coated albumin microcapsules reduce bleeding in severely thrombocytopenic rabbits. Nature Med. 1999; 5:107–11. [PubMed: 9883848]

36. Okamura Y, Fujie T, Nogawa M, Maruyama H, Handa M, Ikeda Y, Takeoka S. Haemostatic effects of polymerized albumin particles carrying fibrinogen γ-chain dodecapeptide as platelet substitutes in severely thrombocytopenic rabbits. Transfusion Medicine. 2008; 18:158–66. [PubMed: 18598278]

37. Bertram JP, Williams CA, Robinson R, Segal SS, Flynn NT, Lavik EB. Intravenous Hemostat: Nanotechnology to Halt Bleeding. Sci Trans Med. 2009; 1:11–22.

38. Spinella PC, Dunne J, Beilman GJ, O'Connell RJ, Borgman MA, Cap AP, Rentas F. Constant challenges and evolution of US military transfusion medicine and blood operations in combat. Transfusion. 2012; 52:1146–53. [PubMed: 22575063]

39. Inaba K, Lustenberger T, Rhee P, Holcomb JB, Blackbourne LH, Shulman I, Nelson J, Talving P, Demetriades D. The impact of platelet transfusion in massively transfused trauma patients. J Am Coll Surg. 2010; 211:573–9. [PubMed: 20846882]

40. Modery-Pawlowski CL, Kuo H-H, Baldwin WM, Sen Gupta A. A platelet-inspired paradigm for nanomedicine targeted to multiple diseases. Nanomedicine. 2013; 8:1709–1727. [PubMed: 24074391]

Essentials

- Platelet transfusion suffers from availability, portability, contamination, and short shelf-life.
- SynthoPlate^{TM} (synthetic platelet technology) can resolve platelet transfusion limitations.
- SynthoPlate^{TM} does not activate resting platelets or stimulate coagulation systemically.
- SynthoPlate^{TM} significantly improves hemostasis in thrombocytopenic mice dose-dependently.

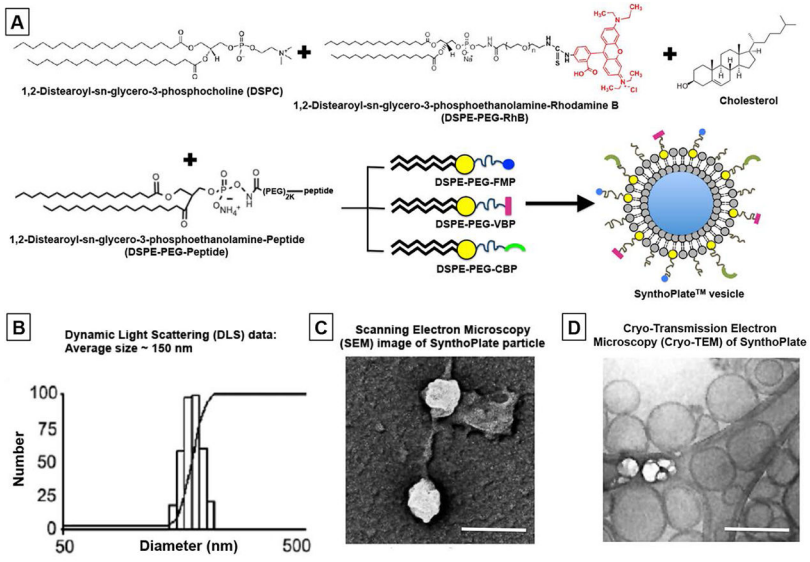

Figure 1.

[A] Schematic representation of SynthoPlate^{TM} manufacture where DSPC, DSPE-PEG-peptides (DSPE-PEG-VBP, DSPE-PEG-CBP and DSPE-PEG-FMP), cholesterol and lipid-RhB were self-assembled at controlled concentrations through reverse phase evaporation and extrusion technique to form heteromultivalently peptide-decorated vesicles; [B] Dynamic Light Scattering (DLS), [C] Scanning Electron Microscopy (SEM) and [D] cryo-Transmission Electron Microscopy (cryo-TEM) characterization of the SynthoPlateTM vesicles exhibit a narrow size distribution, with average diameter ~150 nm; scale bar in [B] and [C] is 200 nm.

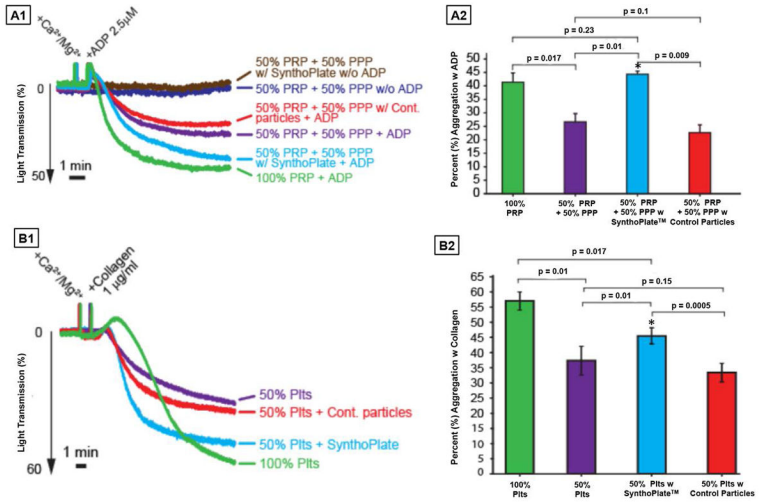

Figure 2.

Representative aggregometry traces (A1 and B1) and corresponding percent (%) platelet aggregation histograms (A2 and B2) of SynthoPlate^{TM} versus control (unmodified) particles with platelet-rich plasma (PRP) using ADP as agonist and washed platelet suspension (Plts) using collagen as agonist; SynthoPlate^{TM} itself does not activate and aggregate resting platelets (brown trace is similar to the indigo trace in A1); Addition of platelet agonist (ADP in A1 and collagen in B1) in 100% PRP or 100% Plts significantly enhances aggregation (green traces in A1 and B1) but this aggregation is significantly decreased if the PRP is 50% diluted with PPP or Plts is 50% diluted with PBS (purple traces innA1 and B1); addition of control (unmodified) particles in the diluting volume of PPP or Plts does not improve this aggregation (red traces A1 and B1), but addition of SynthoPlate^{TM} in the diluting volume of PPP or Plts significantly improves aggregation (cyan traces in A1 and B1); corresponding histograms (A2 and B2) clearly depict the ability of SynthoPlateTM to improve percent (%) aggregation of ADP-activated platelets in 50% diluted PRP and collagen-activated platelets in 50% diluted Plts.

A

GROUPS	Lag time (min)	Time to peak (min)	Max Thrombin Activity (slope/sec)
PPP	20 ± 3.51	24.33 ± 1.86	21.67 ± 1.67
PRP	33.33 ± 1.20	46.33 ± 5.46	22.78 ± 2.42
PPP + SynthoPlate	27.67 ± 3.84	31 ± 3.46	22.22 ± 1.47
PRP + SynthoPlate	34.33 ± 1.86	40.67 ± 1.86	25.56 ± 7.22
PPP + Tissue Factor	1 ± 0	3.33 ± 0.88	77.22 ± 7.47
PRP + Tissue Factor	1 ± 0	3.67 ± 1.20	92.22 ± 2.94
PRP + SynthoPlate + Tissue Factor	1 ± 0	5.33 ± 1.76	88.89 ± 13.14
PRP + ADP + Tissue Factor	1.33 ± 0.33	3.33 ± 0.67	117.22 ± 11.40
PRP + ADP + SynthoPlate + Tissue Factor	1.33 ± 0.33	4 ± 0.57	124.44 ± 9.15

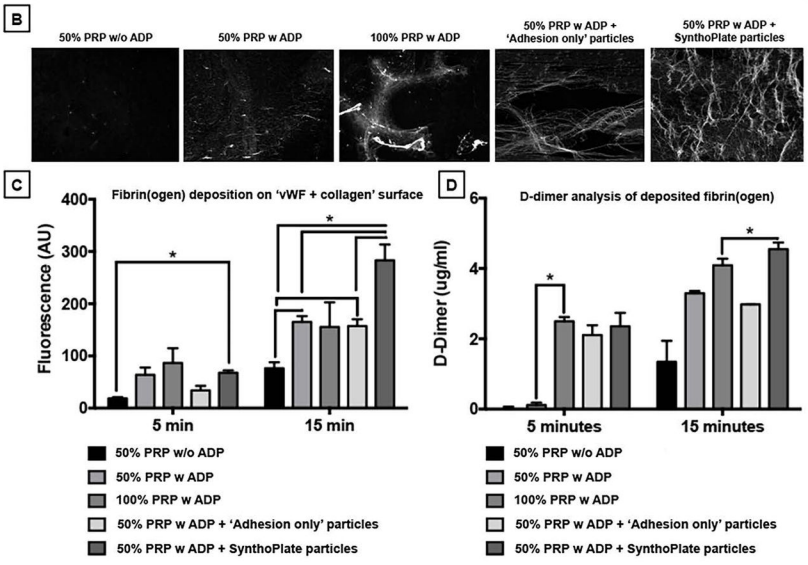

Figure 3.

[A] Table showing results from thrombin generation assay indicates that SynthoPlate^{TM} itself does not have the capability to rapidly activate coagulation factors in plasma to generate thrombin, since just adding SynthoPlate^{TM} to re-calcified PRP or PPP without Tissue Factor (TF) or platelet agonist (e.g. ADP) has no accelerating effect on thrombin generation, and the thrombin generation is enhanced only upon TF and/or ADP addition to PRP or PPP, with SynthoPlate^{TM} slightly enhancing this effect (possibly by recruitment and clustering of active platelets in suspension); [B] Representative fluorescence images at 15 min time-point, as well as, [C] surface-averaged fluorescence intensity values at 5 min and 15 min time-points of fibrin(ogen) generation/deposition on 'vWF + collagen' surface in the PPFC experiments show that, resting platelets (w/o ADP) in 50% PRP (diluted by PPP) generate/deposit only minimal levels of fibrin(ogen) as they interact with the 'vWF + collagen' surface and this generation/deposition increases if platelet agonist is introduced in the flow (i.e. w ADP); introducing SynthoPlateTM vesicles in the flow along with ADP-activated platelets in 50% PRP significantly enhances the fibrin(ogen) generation/deposition during the 15 min flow period, compared to flow with 'adhesion only' particles (control) and

even compared to flow of 100% PRP (w ADP) without SynthoPlate™; [D] D-dimer analysis of the generated/deposited clots on the 'vWF + collagen' surface confirms that the enhanced clot formation in the SynthoPlate™-added group is indeed rich in fibrin and not just fibrinogen binding to recruited active platelets.

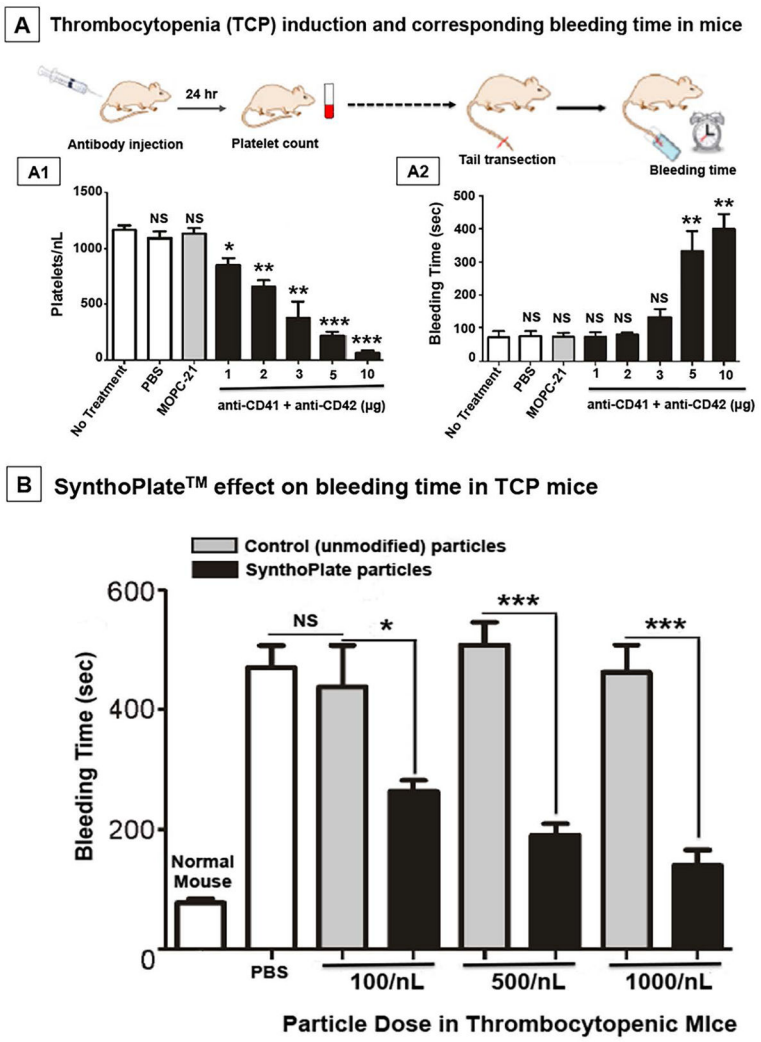

Figure 4.

[A] Experimental design for antibody-induced thrombocytopenia in mice and subsequent tail bleeding studies, where [A1] dose-dependent depletion of platelets resulted in [A2] corresponding increase in bleeding time after tail-transection (10µg antibody cocktail dose resulted in ~90% platelet depletion and corresponding 4–5 fold increase in bleeding time compared to normal mice); [B] Severely thrombocytopenic (TCP) mice injected with PBS or control (unmodified) particles at various doses show no improvement (reduction) of bleeding time, but TCP mice injected with SynthoPlate™ vesicles show a dose-dependent significant improvement of bleeding time, with the highest dose (1000/nL, equivalent to normal murine platelet count) reducing the bleeding time to ~150 sec (close to bleeding time of ~100 sec for normal mice shown for comparison); '*' indicates $p \leq 0.05$, '**' indicates $p \leq 0.01$ and '***' indicates $p \leq 0.001$. NS: Not significant.

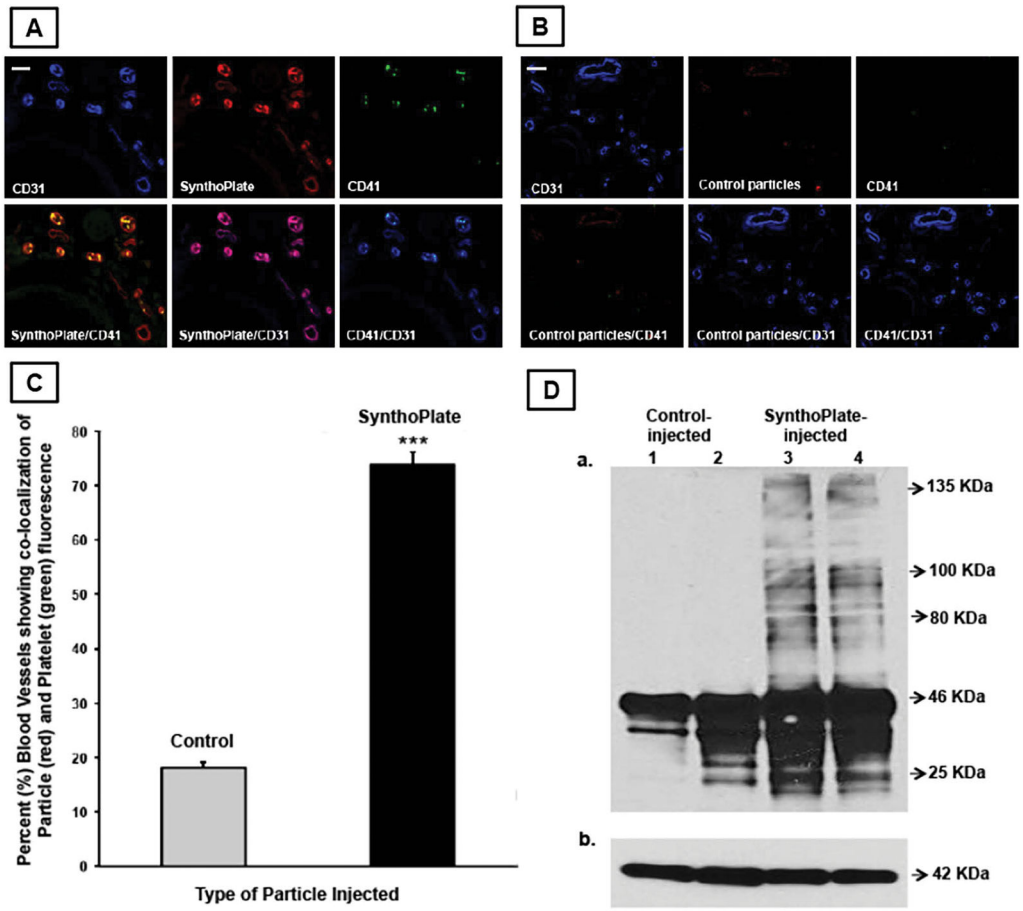

Figure 5.

Representative immunofluorescence microscopy images of tail tissue cryo-sections (transverse section) proximal to hemostasized injury site showing vascular endothelium (blue CD31), particles (red RhB), platelets (green CD41), and corresponding overlays, indicate that [A] tail tissues from SynthoPlate^{TM}-injected mice have significant co-localization of endothelium, particles and platelet fluorescence, while [B] that from control particle-injected mice show minimal co-localization, representative scale bar 25μ; [C] percent (%) of blood vessels showing significant co-localization of particle fluorescence (red) and platelet fluorescence (green) was significantly higher in SynthoPlate^{TM}-injected TCP mice versus control (unmodified) particle-injected mice; ('***' indicates $p \leq 0.001$); [D] immunoblot analysis of injured tail tissue from SynthoPlate^{TM}-treated TCP mice shows a significantly higher presence of high molecular weight fibrin, compared to that from control particle-treated TCP mice.

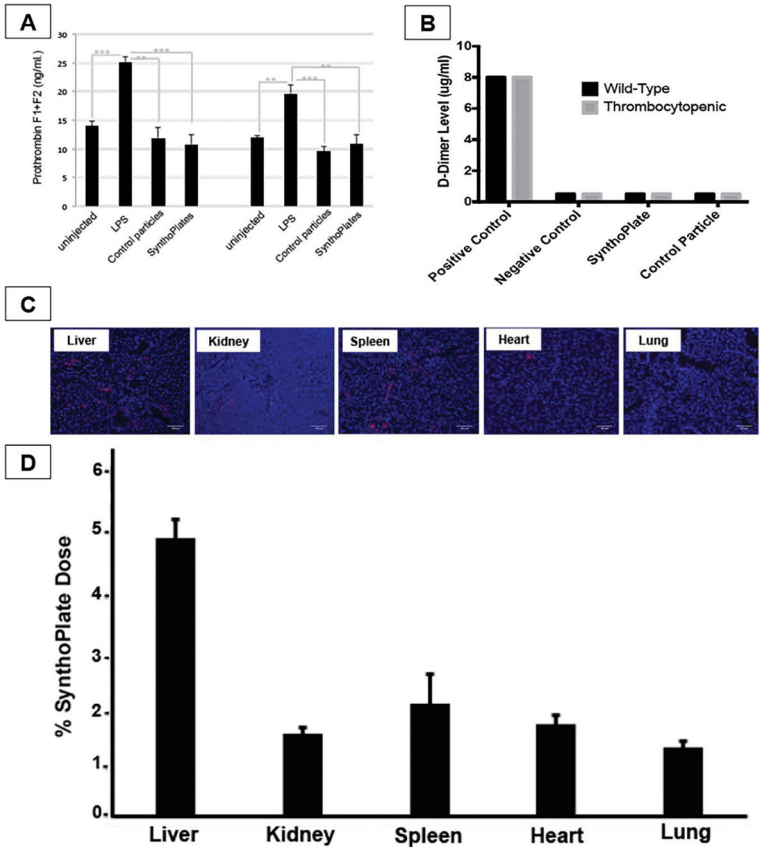

Figure 6.

[A] Prothrombin F1 + F2 fragment ELISA assay, as well as, [B] Stago D-dimer assay in mice injected with SynthoPlate^{TM} indicate that SynthoPlate^{TM} vesicles do not trigger spontaneous formation of thrombin and fibrin in plasma (minimal systemic pro-coagulant risk); [C] Representative fluorescent images (blue: DAPI-stained nuclei, red: Rh-B labeled particles) of harvested tissue cryo-sections and [D] histogram showing systemic localization of SynthoPlate^{TM} vesicles in TCP mice at the 2 hr circulation period indicate that ~15% of injected dose is cleared during the 2 hr period, with liver and spleen being the principal organs of vesicle clearance, with much reduced clearance in kidney, heart and lungs.